

Ray tracing of ion cyclotron waves
in tokamak plasmas

Marco Brambilla

IPP 4/210

March 1983



MAX-PLANCK-INSTITUT FÜR PLASMAPHYSIK

8046 GARCHING BEI MÜNCHEN

MAX-PLANCK-INSTITUT FÜR PLASMAPHYSIK
GARCHING BEI MÜNCHEN

Ray tracing of ion cyclotron waves
in tokamak plasmas

Marco Brambilla

IPP 4/210

March 1983

*Die nachstehende Arbeit wurde im Rahmen des Vertrages zwischen dem
Max-Planck-Institut für Plasmaphysik und der Europäischen Atomgemeinschaft über die
Zusammenarbeit auf dem Gebiete der Plasmaphysik durchgeführt.*

IPP 4/210

Ray tracing of ion cyclotron waves
in tokamak plasmas

Marco Brambilla

March 1983

Abstract

With the present report we begin the presentation of a numerical code, RAYIC, which has been developed with the purpose of applying ray tracing methods to the study of ion cyclotron heating of large tokamak plasmas. This report discusses the theory and displays the equations used by the code. In addition to a presentation of the Eikonal approximation and its use for the description of waves in axisymmetric plasmas of arbitrary meridian cross-section shape, the report contains a summary of a simplified antenna model, and of a treatment of the singular layers (two-ion hybrid and/or cyclotron resonances) where most of the absorption is expected.

This report has been prepared under the contract JB1/9020 between the IPP-EURATOM Association and JET.

C O N T E N T

	page
1. Introduction	2
2. The Eikonal approximation	4
3. Ray tracing in tokamaks	7
4. The dispersion relation of ion cyclotron waves	11
5. Description of the equilibrium	16
6. The ray equations in ψ, θ coordinates.	21
7. Coupling, and boundary values for ray tracing.	28
8. Wave behaviour near singular surfaces	32
9. Discussion	36
References	39
Figure Captions	41

1. Introduction

RAYIC is a numerical code for the study of the propagation and absorption of ion cyclotron waves in large tokamaks of arbitrary cross-section, using the methods of geometric optics /1/. In the present report, we describe the physical model used for this study. In a companion report the structure of the code will be presented, together with the instructions for its use. Finally, a third report will rassemble some examples.

For a reliable description of h.f. plasma heating, a solution of Maxwell equations in the real plasma geometry is required. In the case of a tokamak plasma, the dielectric tensor depends on density and temperature, which are functions only of the magnetic surface, on the one hand; and on the magnetic field intensity, which is a function of the distance from the vertical axis on the other hand. This combined dependence, together with the presence of the rotational transform, is such that a representation of the h.f. fields in terms of normal modes with separate variables is not realizable. On the other hand, in large devices, such as JET, even at the relatively low frequencies in the ion cyclotron resonance domain, the average wavelength is short compared to the plasma dimensions,

$$(1) \quad k_{\perp} a \approx \frac{\omega_{pi}}{c} a \gg 1$$

where k_{\perp} is the wavevector component perpendicular to the static magnetic field, a the plasma radius, and ω_{pi} the ion plasma frequency. Moreover, under appropriate conditions, a substantial fraction of the launched power is absorbed in a single transit through the resonance layers in the plasma. Under these conditions, the Eikonal approximation provides a powerful tool for the approximate solution of the problem of wave propagation. This method, introduced in section 2, and specialized in section 3 to the Tokamak geometry, reduces the solution of Maxwell to the integration of a set of ordinary differential equations, namely the ray equations of geometric optic, and the equation describing the transport of power along the rays.

To write these equations explicitly, two ingredients are required: the dispersion relation of the waves in the frequency range of interest, and an adequate description of the plasma equilibrium. These topics are discussed in sections 4 and 5, respectively. Thus in section 6 the basic set of equations which is integrated by the RAYIC code is presented.

The Eikonal approximation alone is not sufficient for the evaluation of the power deposition profiles in the plasma. In the first place, a set of suitable boundary conditions has to be specified. This requires some information on the field pattern radiated by the antenna. For this purpose, we have incorporated in the code a model of the antenna which is described in section 7.

At the other end of the computation, the difficulty arises that the Eikonal approximation often breaks down precisely near the singular surfaces (ion cyclotron resonances and/or two-ion hybrid resonances) where most of the absorption is likely to occur. A separate investigation of the behaviour of the waves near these singularities is therefore necessary. A summary of these investigations is presented in section 8.

While the description of the code itself will be the subject of a separate report, it is worth mentioning here that the subroutines dealing with the boundary conditions near the antenna, and with the power absorption at resonances, have been conceived as "peripherals", essentially independent from the core of the program. Thus if a more sophisticated antenna model is desired, or a better theory of the resonance surfaces becomes available, these subroutines can be changed without interfering with the main part of the code.

It would be completely misleading to pretend that ray tracing, even supplemented by a separate treatment of the antenna and of the resonance layers, can satisfactorily describe every ion cyclotron heating scenario in large plasmas. Section 9 will be devoted to a discussion of the limits of the ray-tracing approach. This section should to some extent play the role of a summary of the present status of the theory, for the hurried reader not interested in the details of sections 2 to 8.

The circumstance that ray tracing is far from providing a complete description of how ion cyclotron heating will work is perhaps disappointing, and the question could be raised whether some more comprehensive theoretical approach should be preferred. Unfortunately, no such approach is available at present, and it will take some time to develop one. On the other hand, provided its limitations are not overlooked, ray tracing can be of great help in understanding ion cyclotron heating.

In the course of this work we have benefitted from the help of several people. Our first investigations of the application of ray tracing to toroidal plasma have been undertaken in collaboration with A. Cardinali /1/. The antenna model is heavily indebted to the work of K. Teilhaber, G. Lister, and J. Jacquinet /2/. The wave behaviour near singular surfaces is being studied by M. Ottaviani and the present author. Where appropriate, the results of these studies will be separately published in more details.

Finally, we wish to thank O. Debarbieri, who has provided a predictor-corrector subroutine for the integration of ordinary differential equations, particularly appropriate for the application to ray-tracing.

2. The Eikonal approximation

The Eikonal approximation for waves in magnetized plasma has been discussed by Weinberg /3/ and Bernstein /4/; its application to waves in toroidally confined plasmas has been further investigated by Brambilla and Cardinali /1/. For completeness, we recall here the basic equations of the theory and their meaning, without rigorous justification.

Anticipating that the fields are expected to be locally similar to plane waves with slowly varying wavevector \vec{k} , the basic assumptions of the Eikonal theory can be stated as follows:

a) the length characterizing the non-locality (dispersion) of the dielectric tensor is short compared to the wavelength:

$$(1) \quad \frac{k_{\perp}^2 v_{thi}^2}{\Omega_{ci}^2} \ll 1$$

$$(2) \quad \left| \frac{\omega - n \Omega_{ci}}{k_{\parallel} v_{thi}} \right| \gg 1 \quad n = 0, \pm 1, \pm 2 \dots$$

for all the species of charged particles (parallel and perpendicular refer to the direction of the static magnetic field, v_{th} and Ω_c are the thermal velocity and cyclotron frequency, respectively).

b) the dielectric tensor varies only moderately over a wavelength, so that for example

$$(3) \quad k^{-2} |\text{div } \vec{k}| \ll 1$$

c) The antihermitean part of the dielectric tensor is small compared to the hermitean part

$$(4) \quad |\varepsilon_{ij}^A| \ll |\varepsilon_{ij}^H|$$

(i.e. the fractional absorption per wavelength is moderate).

Under these conditions, a solution to Maxwell equations is sought in the form

$$(5) \quad \vec{E} = \vec{E}_{\vec{k}}(\vec{r}) e^{i(S(\vec{r}) - \omega t)}$$

where it is assumed that the amplitude $\vec{E}_{\vec{k}}$ and the (real) "local wavevector"

$$(6) \quad \vec{k}(\vec{r}) = \vec{\nabla} S$$

are slowly varying functions. Substituting (5) into Maxwell equations and collecting the largest terms, one obtains in the usual way the local dispersion relation

$$(7) \quad H(\vec{k}, \vec{r}) \equiv \det \left| \frac{c^2}{\omega^2} (k_i k_j - \delta_{ij} k^2) - \epsilon_{ij}^H \right| = 0$$

(we omit the frequency dependence; the antihermitean part of ϵ is neglected because of assumption c)). Equation (7) is a partial differential equation for the Eikonal function S ; its characteristics are the ray equations of geometric optics

$$(8) \quad \frac{d\vec{r}}{d\tau} = \frac{\partial H}{\partial \vec{k}} \quad \frac{d\vec{k}}{d\tau} = -\frac{\partial H}{\partial \vec{r}}$$

The parameter τ has no immediate significance; this form of the ray equations has however the advantage of being explicitly Hamiltonian. If a ray is followed by integrating Eqs. (8) with initial conditions (\vec{k}_0, \vec{r}_0) satisfying (7), the dispersion relation remains satisfied throughout, since

$$(9) \quad \frac{dH}{d\tau} = \frac{\partial H}{\partial \vec{k}} \cdot \frac{d\vec{k}}{d\tau} + \frac{\partial H}{\partial \vec{r}} \cdot \frac{d\vec{r}}{d\tau} = 0$$

At the same time, the evaluation of the phase S reduces to a quadrature:

$$(10) \quad S(\vec{r}) = S(\vec{r}_0) + \int_{\tau_0}^{\tau} \left(\vec{k} \cdot \frac{d\vec{r}}{d\tau} \right) d\tau$$

Finally, the identical vanishing of the determinant (7) allows the determination of the field polarization at each point, i.e. of the unit polarization vector

$$(11) \quad \vec{e}_k = \frac{\vec{E}_k(\vec{r})}{|\vec{E}_k(\vec{r})|} \quad \vec{e}_k^* \cdot \vec{e}_k \equiv 1$$

The surfaces $\Sigma : S(\vec{r}) = \text{cte}$ are the "wavefronts". By definition, \vec{k} is everywhere perpendicular to the wavefront. For ray tracing to produce meaningful approximate solutions of Maxwell equations, the linear dimensions and the radius of curvature of wavefront must be large compared to the local wavelength; only then diffraction effects can be neglected. This is also the condition for concepts such as local wave-vector, group velocity, or power flux through the ray pencil, to have a physical content. Finally, it is clear that the knowledge of an initial wavefront Σ_0 , together with the dispersion relation, completely specifies a set of initial conditions for the ray equations (8).

To close the Eikonal approximation, the ray equations have to be supplemented with an equation for the slowly varying amplitude $|\vec{E}_k|$, or, equivalently, for the transport of energy. This equation is conveniently written in the form of a generalized Poynting theorem:

$$(12) \quad \text{div } \vec{S}_k = -2\gamma_k \frac{c|\vec{E}_k|^2}{16\pi}$$

$$(13) \quad \vec{S}_k = \frac{c^2}{8\pi\omega} \text{Re} \left[\vec{E}_k^* \times (\vec{k} \times \vec{E}_k) \right] - \frac{\omega}{16\pi} \vec{E}_k^* \cdot \frac{\partial \underline{\underline{\epsilon}}^H}{\partial \vec{k}} \cdot \vec{E}_k$$

$$(14) \quad \gamma_k = \vec{e}_k^* \cdot \underline{\underline{\epsilon}}^A \cdot \vec{e}_k$$

\vec{S}_k is the energy flux, including the contribution from the coherent response of the particles to the waves. The r.h.s. of Eq. (12) takes into account dissipation. It is easily shown that

$$(15) \quad 2\gamma_k \frac{c}{16\pi} |\vec{E}_k|^2 = \frac{d}{dt} \sum_{\text{spec}} \int \frac{m v^2}{2} f(\vec{v}) d\vec{v}$$

The amount of power absorbed by each species is also immediately determined by decomposing $\underline{\underline{\epsilon}}^A$ into the contributions from the different kinds of charged particles.

3. Ray Tracing in Tokamaks

In an axisymmetric plasma, a further simplification follows from the fact that the coordinate φ is "ignorable", hence

$$(1) \quad m_\varphi = \frac{\partial S}{\partial \varphi} = \text{cte}$$

Thus

$$(2) \quad S(\vec{r}) = \sigma_{m_p}(\vec{\rho}) + n_\phi \cdot \phi$$

and

$$(3) \quad \vec{k} = \vec{\kappa}_p(\vec{\rho}) + \frac{n_\phi}{R} \vec{e}_\phi$$

$$\kappa_p = \vec{\nabla}_p \sigma_{m_\phi}$$

where $\vec{\rho}$ is the position vector in the meridian plane, and $\vec{e}_\phi = \vec{\nabla}\phi/R$ the unit vector along ϕ , R being the distance from the vertical axis. The subscript p stays for "poloidal". With (1) and (2)-(3), the ray equations reduce to

$$(4) \quad \frac{d\vec{\rho}}{d\tau} = \frac{\partial H}{\partial \vec{\kappa}_p} \quad \frac{d\vec{\kappa}_p}{d\tau} = -\frac{\partial H}{\partial \vec{\rho}}$$

It is important to realize, however, that in this simple form the Eikonal approximation is incompatible with the way I C waves are normally excited.

Let $\Delta\phi$ and $\Delta\theta$ denote the angular aperture of the antenna (or of an antenna element if several are used) in the toroidal and poloidal direction respectively. $\Delta\phi$ and $\Delta\theta$ also characterize the region over which the field amplitude ($|E_k|$ in Eq. (2-5)) is approximately constant in front of the antenna, where the initial wavefront Σ_0 has to be located. For the validity of the Eikonal approximation $\Delta\phi$ and $\Delta\theta$ should satisfy

$$(5) \quad n_\phi \cdot \Delta\phi \gg 1 \quad \left(\frac{\omega}{c} R \cdot \Delta\phi \gg 1 \text{ if } n_\phi \approx 0 \right)$$

$$(6) \quad a \kappa_p \cdot \Delta\theta \gg 1$$

where a is the plasma radius. Due to the large refractive index of the fast wave, condition (6) can usually be satisfied by choosing the initial wavefront at a layer where the plasma density is already sufficiently

large. On the other hand the dimensions of the antenna in the toroidal direction are usually far too small to make it possible to satisfy condition (5).

The difficulty can be overcome by representing the total field as a superposition of the form

$$(7) \quad \vec{E}(\vec{r}) = \sum_{n_\varphi} \vec{E}_{n_\varphi}(\vec{\rho}) \exp i [\sigma_{n_\varphi}(\vec{\rho}) + n_\varphi \cdot \varphi - \omega t]$$

$$n_\varphi = 0, \pm 1, \pm 2, \dots$$

and applying ray tracing separately to each partial wave. Since the amplitudes $\vec{E}_{n_\varphi}(\vec{\rho})$ do not depend on φ , condition (6) is automatically satisfied. On the other hand, by choosing the amplitudes \vec{E}_{n_φ} appropriately, it is always possible to reproduce the field launched by any antenna configuration.

The price paid for this enlargement of the scope of ray tracing is that the explicit evaluation of the total field (7) becomes exceedingly tedious. If the goal is the investigation of plasma heating, however, such an evaluation is not required: the information obtained from ray tracing about each partial wave separately ($k_{||}$ and k_{\perp} at each point, occurrence of reflections, etc.) is more directly relevant than the knowledge of the total field. This is because the flux of energy P_{Σ_p} through any axisymmetric surface Σ_p (such as a strip of wavefront Σ_0) reduces to the sum of the contributions from each partial wave separately. Indeed (evaluating P_{Σ_p} at the plasma edge, where only the electromagnetic contribution is present)

$$(8) \quad P_{\Sigma_p} = \int_{\Sigma_p} \int_0^{2\pi} d\varphi \cdot \frac{c}{8\pi} \operatorname{Re}(\vec{E}^* \times \vec{B}) \cdot d\vec{\Sigma}_p =$$

$$= \frac{c}{8\pi} \operatorname{Re} \left\{ \sum_{n_\varphi} \int_{\Sigma_p} [\vec{E}_{n_\varphi}^* \times (\vec{k} \times \vec{E}_{n_\varphi})] \cdot d\vec{\Sigma}_p \right\} = \sum_{n_\varphi} P(n_\varphi)$$

By integrating Eq. (2-13) over a portion of ray pencil bounded by two wavefronts separated by a small phase difference $d\sigma$, the equation for

energy transport can be cast in the form

$$(9) \quad \frac{dP(m_p)}{d\sigma} = - \frac{\gamma_{\vec{k}}}{(c \vec{\kappa}_p \cdot \vec{l}_k / \omega)} P(m_p)$$

where $\gamma_{\vec{k}}$ is given by Eq. (2-14) and

$$(10) \quad \vec{T}_{\vec{k}} = \frac{c}{\omega} \left[\vec{k} - \vec{e}_k^* (\vec{k} \cdot \vec{e}_k) \right] - \frac{j\omega}{2c} \vec{e}_k^* \cdot \frac{\partial \varepsilon^H}{\partial \vec{k}} \cdot \vec{e}_k$$

Equation (9) can be integrated simultaneously with the ray equations, with the spectral distribution of the power radiated by the antenna as initial condition; this allows the explicit evaluation of the radial power deposition profile.

Equation (9) also suggests a natural choice of the independent variable for ray tracing, namely the poloidal phase σ itself. The change from τ to σ is simply performed by dividing both sides of Eqs. (4) with

$$(11) \quad \frac{d\sigma}{dz} = \vec{\kappa}_p \cdot \frac{\partial H}{\partial \vec{\kappa}_p}$$

With this choice of the independent variable, for example, the graphical display of successive wavefronts along a ray pencil is much simplified, and provides a very useful visual summary of the wave behaviour. It is moreover shown in /1/ that the vanishing of $d\sigma/d\tau$ is the most common occurrence of a breakdown of the Eikonal approximation. With σ as independent variable, the integration of the ray equations is automatically stopped in such cases, thus ensuring that the approximation is not used beyond its domain of validity. It is perhaps not superfluous to stress here that the frequently preferred choice of the time of transit of signals as independent variable (implemented by dividing Eqs. (4) with $dt/d\tau = -\partial H/\partial \omega$) is not only numerically inconvenient, but completely pointless when dealing with a steady-state situation.

4. The dispersion relation of ion cyclotron waves

The dispersion relation of waves in the ion cyclotron frequency range has been the object of a long series of investigations; for a summary, we refer to Brambilla /5/. The complete dispersion relation for a Vlasov plasma is needlessly complicated; its use would make ray tracing quite slow. A development for small Larmor radius and small electron inertia gives an accurate approximation, including all the relevant physics, but sufficiently simple for computational purposes:

$$(1) \quad H(\omega, \vec{k}, \vec{r}) = A n_{\perp}^4 - B n_{\perp}^2 + C$$

$$A = \frac{1}{2}(\lambda + \rho) + \tau = \sigma_{\perp}$$

$$(2) \quad B = -[(n_{\parallel}^2 - S) + (n_{\parallel}^2 - R)\lambda + (n_{\parallel}^2 - L)\rho]$$

$$C = (n_{\parallel}^2 - R)(n_{\parallel}^2 - L)$$

Here $\vec{n} = \vec{k}c/\omega$; the other quantities are defined as follows:

$$(3) \quad S = \frac{1}{2}(R + L)$$

$$R = 1 + \frac{\omega_{pe}^2}{\Omega_e^2} - \sum_j \frac{\omega_{pj}^2}{\omega^2} \left(\frac{\omega}{\omega + \Omega_j} - \frac{\omega}{\Omega_j} \right)$$

$$L = 1 + \frac{\omega_{pe}^2}{\Omega_e^2} - \sum_j \frac{\omega_{pj}^2}{\omega^2} \left(-x_{oj} \zeta_R(x_{ij}) + \frac{\omega}{\Omega_j} \right)$$

$$\rho = \frac{1}{2} \sum_j \frac{\omega_{pj}^2}{\Omega_{cj}^2} \frac{v_{thj}^2}{c^2} \left\{ 1 - 2 \frac{\omega}{\omega + \Omega_j} + \frac{\omega}{\omega + 2\Omega_j} \right\}$$

$$\lambda = \frac{1}{2} \sum_j \frac{\omega_{pj}^2}{\Omega_{cj}^2} \frac{v_{thj}^2}{c^2} \left\{ 1 - 2(-x_{oj} \zeta_R(x_{ij})) + (-x_{oj} \zeta_R(x_{2j})) \right\}$$

$$\tau = \frac{1}{2} \sum_j \frac{\omega_{pj}^2}{\Omega_{cj}^2} \frac{v_{thj}^2}{c^2} \left\{ -1 + \frac{1}{2} \left[(-x_{oj} \zeta_R(x_{ij})) + \frac{\omega}{\omega + \Omega_j} \right] \right\}$$

The summation extends over the species of ions; the other notations are standard:

$$\omega_p^2 = \frac{4\pi n e^2 Z^2}{m} \quad \Omega_c = \frac{ZeB}{mc}$$

$$(4) \quad v_{th}^2 = 2T/m$$

$$\alpha_{nj} = \frac{\omega - n\Omega_{cj}}{k_{\parallel} v_{thj}} \quad n = 0, \pm 1, \pm 2$$

$$(5) \quad Z(x) = \frac{1}{\sqrt{\pi}} P \int \frac{e^{-u^2}}{u - x} du + i\sqrt{\pi} e^{-x^2}$$

(only the real part of Z is taken into account in writing H ; the imaginary part enters in the evaluation of ϵ^A , cfr. below).

Equation (1) describes two waves: the fast (extraordinary, or compressional Alfvén) wave, with approximate dispersion relation

$$(6) \quad n_{\perp}^2 = Q_F^2 = - \frac{(n_{\parallel}^2 - R)(n_{\parallel}^2 - L)}{(n_{\parallel}^2 - S)}$$

and the lowest Ion Bernstein wave, with approximate dispersion relation

$$(7) \quad n_{\perp}^2 = Q_B^2 = - \frac{(n_{\parallel}^2 - S)}{\sigma_i}$$

It does not describe the slow cold plasma wave (ordinary or Shear Alfvén wave): this omission is justified whenever the plasma pressure is not too low,

$$(8) \quad \beta = \frac{8\pi n T}{B_0^2} \gtrsim m_e/m_i$$

(m_e, m_i being the electron and ion masses, respectively). In a large Tokamak, this condition is usually violated only close to the plasma edge, where the Eikonal approximation is anyhow non valid, and the role of ray tracing is taken over by the theory of the antenna.

The other "singular surfaces", on which the Eikonal approximation is bound to breakdown, are easily identified by inspection of Eq. (1). They are

a) the fundamental and first harmonic of the ion cyclotron resonances

$$(9) \quad \omega = \Omega_j \quad \omega = 2\Omega_j$$

Here the antihermitean part of the dielectric tensor becomes comparable to the hermitean part;

b) the two-ion resonances in multispecies plasmas (confluence of the fast and Bernstein waves at $n_{||}^2 - S \approx 0$, cut-off at $n_{||}^2 = L$). In the so-called "minority" regime, when the concentration of the minority species is small, the two-ion hybrid resonance can merge with the Doppler-broadened ion cyclotron resonance of the minority species itself;

c) in a single species plasma near $\omega = 2\Omega_j$ a similar cut-off-confluence pair occurs, due to the locally large value of σ_1 . In this case too, the confluence merges with the cyclotron resonance if $k_{||}$ is sufficiently large.

Since most of these failures of ray tracing occur near or coincide with the layers of strong absorption, it is often necessary to make a separate study of the behaviour of waves impinging on such layers. The present status of these investigations is summarized in Section 8.

From Brambilla (1982) we also cite the expressions for the components of the unit polarization vector \vec{e}_k (Eq. 2-11), which are needed to write in explicit form the energy transport equation. Introducing a local "Stix" reference frame x, y, z with z along the static magnetic field B_0 , and x in the direction of $\vec{k}_\perp = \vec{k} - (\vec{k} \cdot \vec{B}_0) \vec{B}_0 / B_0^2$, we have

$$e_x = \frac{1}{\sqrt{2}}(e_+ + e_-) \quad e_y = -\frac{i}{\sqrt{2}}(e_+ - e_-)$$

$$(10) \quad \begin{aligned} e_+ &= K_e \left[R - (\rho - \varepsilon) n_\perp^2 - n_\parallel^2 \right] \\ e_- &= K_e \left[L - (\lambda - \varepsilon) n_\perp^2 - n_\parallel^2 \right] \\ e_z &= -K_e n_\perp n_\parallel \frac{S - \sigma n_\perp^2 - (n_\parallel^2 + n_\perp^2)}{P - n_\perp^2} \end{aligned}$$

where

$$(11) \quad P = -\frac{\omega_{pe}^2}{\omega^2} x_{oe}^2 Z'_R(x_e)$$

and K_e is the normalization constant required to make $(\vec{e}_k \cdot \vec{e}_k) = 1$.

In the "Stix" frame, the components of the vector \vec{T}_k (Eq. 10) are

$$(12) \quad \begin{aligned} T_x &= \frac{c}{\omega} \left\{ k_\perp - e_x (k_\perp e_x + k_\parallel e_z) + \right. \\ &\quad \left. + k_\perp (\lambda |e_+|^2 + \rho |e_-|^2 + 2\varepsilon e_+ e_-) \right\} \end{aligned}$$

$$T_y = 0$$

$$\begin{aligned} T_z &= \frac{c}{\omega} \left\{ k_\parallel - e_z (k_\perp e_x + k_\parallel e_z) + \right. \\ &\quad \left. - \frac{1}{2} \frac{\omega^2}{c^2} \left[\left(\frac{\partial L}{\partial k_\parallel} - n_\perp^2 \frac{\partial \lambda}{\partial k_\parallel} \right) |e_+|^2 - 2 \frac{\partial \varepsilon}{\partial k_\parallel} e_+ e_- + \frac{\partial P}{\partial k_\parallel} |e_-|^2 \right] \right\} \end{aligned}$$

Finally, we write down the quantity $\gamma_{\vec{k}} = \gamma_{\vec{k}}^{(e)} + \sum_j \gamma_{\vec{k}}^{(j)}$ describing the dissipation, decomposed into the contributions from the electrons and each species of ions: For the electrons:

$$\gamma_{\vec{k}}^{(e)} = \gamma_{\vec{k}}^{(ELD)} + \gamma_{\vec{k}}^{(TTHP)}$$

$$(13) \quad \gamma_{\vec{k}}^{(ELD)} = 2\sqrt{\pi} \frac{\omega_{pe}^2}{\omega^2} x_{oe}^3 e^{-x_{oe}^2} |e_z|^2$$

$$\gamma_{\vec{k}}^{(TTHP)} = \sqrt{\pi} n_{\perp}^2 \beta_e x_{oe} e^{-x_{oe}^2} |e_y|^2$$

where $\beta_e = \frac{\omega_{pe}^2}{\Omega_e^2} \frac{v_{the}^2}{c^2} = \frac{8\pi n_e e^2}{B_e}$

The first term here describes parallel Landau Damping, the second Transit Time Magnetic Pumping by the electrons. Due to the large values of n_{\perp}^2 and of the ratio $|e_y|^2/|e_z|^2$, the latter is usually a much more efficient mechanism for electron heating. For the ions we have

$$\gamma_{\vec{k}}^{(i)} = \gamma_{\vec{k}}^{(0)} + \gamma_{\vec{k}}^{(1)}$$

$$(14) \quad \gamma_{\vec{k}}^{(0)} = \sqrt{\pi} x_{oj} e^{-x_{oj}^2} \frac{\omega_{pj}^2}{\omega^2} \left\{ \left(1 - \frac{k_{\perp}^2 v_{thj}^2}{\Omega_j^2} \right) |e_+|^2 + \right.$$

$$\left. + \frac{1}{2} \frac{k_{\perp}^2 v_{thj}^2}{\Omega_j^2} |e_+ + e_-|^2 \right\}$$

$$\gamma_{\vec{k}}^{(1)} = \sqrt{\pi} x_{oj} e^{-x_{oj}^2} \cdot \frac{1}{2} \frac{\omega_{pj}^2}{\omega^2} \frac{k_{\perp}^2 v_{thj}^2}{\Omega_j^2} |e_+|^2$$

representing the contribution from the fundamental and the first harmonic of the cyclotron resonance, respectively.

5. Description of the equilibrium

Let X, Z be orthogonal coordinates in any meridian plane, with X horizontal and Z vertical, and with origin on the magnetic axis $R = R_0$. The set of magnetic surfaces is parametrically described by the equations

$$(1) \quad X = X(\psi, \vartheta) \quad Z = Z(\psi, \vartheta)$$

The variable ψ labels magnetic surfaces; it is arbitrarily normalized so that

$$(2) \quad 0 \leq \psi \leq 1$$

($\psi = 0$ on the magnetic axis, $\psi = 1$ on the plasma surface); ϑ is the usual poloidal angle (Fig. 1).

The unit vectors parallel and perpendicular to the magnetic surface in the meridian plane are

$$\begin{aligned} \vec{e}_\vartheta &= -\sin \vartheta \vec{e}_X + \cos \vartheta \vec{e}_Z \\ (3) \quad \vec{e}_\psi &= \vec{e}_\vartheta \times \vec{e}_\phi = \cos \vartheta \vec{e}_X + \sin \vartheta \vec{e}_Z \\ \cos \vartheta &= \frac{1}{N_\vartheta} \frac{\partial Z}{\partial \theta} \quad \sin \vartheta = -\frac{1}{N_\vartheta} \frac{\partial X}{\partial \theta} \end{aligned}$$

$$(4) \quad N_\vartheta^2 = \left(\frac{\partial X}{\partial \theta} \right)^2 + \left(\frac{\partial Z}{\partial \theta} \right)^2$$

It is also convenient to define an angle σ such that

$$(5) \quad \vec{e}_\theta = -\sin \sigma \vec{e}_X + \cos \sigma \vec{e}_Z$$

$$(6) \quad \cos \sigma = \frac{1}{N_\sigma} \frac{\partial X}{\partial \psi} \quad \sin \sigma = \frac{1}{N_\sigma} \frac{\partial Z}{\partial \psi}$$

$$N_\sigma^2 = \left(\frac{\partial X}{\partial \psi} \right)^2 + \left(\frac{\partial Z}{\partial \psi} \right)^2$$

Thus

$$(7) \quad \vec{\nabla} \psi = \frac{N_\sigma}{J} \vec{e}_\psi \quad \vec{\nabla} \theta = \frac{N_\sigma}{J} \vec{e}_\theta$$

$$(8) \quad \vec{\nabla} \psi \cdot \vec{\nabla} \theta = -G/J^2$$

where

$$(9) \quad J = \frac{\partial X}{\partial \psi} \frac{\partial Z}{\partial \theta} - \frac{\partial X}{\partial \theta} \frac{\partial Z}{\partial \psi} = N_\sigma N_\epsilon \cos(\sigma - \epsilon)$$

$$(10) \quad G = \frac{\partial X}{\partial \psi} \frac{\partial X}{\partial \theta} + \frac{\partial Z}{\partial \psi} \frac{\partial Z}{\partial \theta} = N_\sigma N_\epsilon \sin(\sigma - \epsilon)$$

Note that

$$(11) \quad J^2 = N_\sigma^2 N_\epsilon^2 - G^2$$

When the equilibrium is given in the form (1), the variables (ψ, θ, φ) are naturally used to implement ray tracing. Their metric tensor is

$$(12) \quad g_{ik} = \begin{vmatrix} N_\sigma^2 & G & 0 \\ G & N_\epsilon^2 & 0 \\ 0 & 0 & R^2 \end{vmatrix}$$

The fact that in general $G \neq 0$ implies that these coordinates are not orthogonal. (Only if the cross-sections of the magnetic surfaces are concentric circles it is easily seen that $\sigma = \tau = \vartheta$ and $G = 0$.)

The representation (1) implicitly contains also a complete information on the pressure and poloidal field profiles /6/, in a form however inconvenient for rapid computation. Instead, we assume that $p(\psi)$ is known (compatibly with Eq. (1)), and proceed to evaluate $B_p(\psi, \vartheta)$.

The total magnetic field can be written

$$(13) \quad \vec{B} = \frac{R_0}{R} \left\{ \left(a \frac{N_z^2}{J} \right) B_p(\psi) \vec{e}_z + B_T(\psi) \vec{e}_\phi \right\}$$

By taking the curl of this equation, the components of the current density are found to be

$$(14) \quad \frac{4\pi}{c} J_z = - \frac{R_0}{R} \frac{N_z^2}{J} \frac{dB_T}{d\psi}$$

$$(15) \quad \frac{4\pi}{c} J_\phi = \frac{a}{J} \left\{ \frac{\partial}{\partial \psi} \left[\left(\frac{N_z^2 R_0}{J R} \right) B_p(\psi) \right] - \left[\frac{\partial}{\partial \theta} \left(\frac{G R_0}{J R} \right) \right] B_p(\psi) \right\}$$

(the plasma radius a is inserted in the definitions in such a way that the cylindrical limit is most easily obtained; the quantities B_p and B_T must be independent from ϑ to ensure that $\text{div. } \vec{B} = 0$ and $J_\psi = 0$).

By substituting (13) - (15) into the pressure balance equation, we obtain the Grad-Shafranov equation in the form

$$(16) \quad \frac{a^2}{J} B_p(\psi) \left\{ \frac{\partial}{\partial \psi} \left[\left(\frac{N_z^2 R_0}{J R} \right) B_p(\psi) \right] - \left[\frac{\partial}{\partial \theta} \left(\frac{G R_0}{J R} \right) \right] B_p(\psi) \right\} =$$

$$= - \left\{ 4\pi \frac{R_0}{R} \frac{dp}{d\psi} + \frac{R}{R_0} B_T(\psi) \frac{dB_T}{d\psi} \right\}$$

Since $B_p(\psi)$ is independent from ϑ , while the coefficients contain ϑ explicitly, this equation must be regarded as a restriction on the possible form of Eqs. (1). Indeed, Eq. (16) has been used /7/ to find classes of possible equilibria. Here, however, we already suppose that Eqs. (1) describe, albeit possibly only approximatively, a true equilibrium, and are therefore compatible with Eq. (16). Hence we come back to Eq. (15), and we proceed as follows.

The total toroidal current flowing within a magnetic surface ψ is

$$(17) \quad \mathcal{I}(\psi) = \int_{<\psi} (\vec{j} \cdot \vec{\nabla} \phi) dV = \int_0^{2\pi} d\vartheta \int_0^\psi d\psi \int \cdot j_\phi(\psi, \vartheta)$$

We can therefore define an average current density

$$(18) \quad j_\phi^{AVG}(\psi) = \int_0^{2\pi} j \cdot j_\phi(\psi, \vartheta) d\vartheta / S(\psi)$$

$$(19) \quad S(\psi) = \int_0^{2\pi} j d\vartheta$$

($S(\psi)\Delta\psi$ is the area between the magnetic surfaces ψ and $\psi+\Delta\psi$ in the poloidal cross-section) so that

$$(20) \quad \mathcal{I}(\psi) = \int_0^\psi S(\psi) j_\phi^{AVG}(\psi) d\psi$$

It is now natural to assume that $j_\phi^{AVG}(\psi)$ is known, for example that it is proportional to $(T_e(\psi))^{1.5}$, so that (20) can be rewritten

$$(20') \quad \mathcal{I}(\psi) = \mathcal{I}_{TOT} \frac{\int_0^\psi S(\psi) [T_e(\psi)]^{3/2} d\psi}{\int_0^1 S(\psi) [T_e(\psi)]^{3/2} d\psi}$$

By averaging Eq. (15) over the magnetic surface (with weight j/a) we immediately obtain

$$(21) \quad B_p(\psi) = \frac{2}{c} \frac{I(\psi)}{a \Lambda(\psi)}$$

$$(22) \quad \Lambda(\psi) = \frac{1}{2\pi} \int_0^{2\pi} \left(\frac{N_z^2 R_0}{J R} \right) d\vartheta$$

Note that assigning $J_\phi^{AVG}(\psi)$ is equivalent to assign the second arbitrary function $B_T(\psi)$ in the r.h.s. of the Grad-Shafranov equation, since by averaging (16) multiplied by R_0/R we have

$$(23) \quad B_T \frac{dB_T}{d\psi} = - \left[4\pi \kappa(\psi) \frac{dp}{d\psi} + B_p(\psi) \frac{d}{d\psi} (\Lambda' B_p(\psi)) \right]$$

$$\kappa(\psi) = \frac{1}{S(\psi)} \int_0^{2\pi} \frac{R_0^2}{R^2} \frac{J}{a^2} d\vartheta$$

$$\Lambda'(\psi) = \frac{1}{S(\psi)} \int_0^{2\pi} \frac{N_z^2 R_0^2}{J R^2} d\vartheta$$

(note that $\Lambda'(\psi) \neq \Lambda(\psi)$ since $\langle J_\phi B_T \rangle \neq \langle J_\phi \rangle \cdot \langle B_T \rangle$).

This equation is, however, difficult to integrate accurately, since it expresses $B_T(dB_T/d\psi)$ as the difference of two almost equal quantities. On the other hand, $B_T(\psi)$ differs from B_0 only by a correction of order $\beta \ll 1$: a negligible error is made by assuming in the ray tracing code that $B_T = B_0$, i.e. that the toroidal field is identical with the vacuum field, $B_\psi = B_0 R_0/R$. The quantities required in the code,

$$(24) \quad \tan \Theta \equiv \frac{B_z}{B_\phi} = \left(\frac{aN_z}{J} \right) \frac{B_p(\psi)}{B_T(\psi)}$$

$$\equiv \left(\frac{aN_z}{J} \right) \frac{2I(\psi)}{ca B_0 \Lambda(\psi)}$$

and

$$(25) \quad \Omega = \Omega_0 \frac{R_0}{R} \sqrt{1 + \tan^2 \Theta}$$

are negligibly affected by this approximation.

The description of the equilibrium, insofar required for the implementation of ray tracing, is thereby complete. We only note that the safety factor $q(\psi)$ in the present notations is given by

$$(26) \quad q(\psi) = \left[\frac{1}{2\pi a} \int_0^{2\pi} \frac{I}{R} d\theta \right] \cdot \frac{B_T(\psi)}{B_P(\psi)}$$

6. The ray equations in ψ, ϑ coordinates

The natural variables for the ray equations in the plasma equilibrium described in the previous section are of course ψ, ϑ , together with the "conjugate" wavevector components

$$(1) \quad \begin{aligned} \tilde{k}_\psi &= \frac{\partial X}{\partial \psi} k_X + \frac{\partial Z}{\partial \psi} k_Z \\ \tilde{k}_\theta &= \frac{\partial X}{\partial \theta} k_X + \frac{\partial Z}{\partial \theta} k_Z \end{aligned}$$

\tilde{k}_ψ and \tilde{k}_θ are the covariant components of \vec{k} in the poloidal plane; the covariant component conjugate to the toroidal angle φ is $\tilde{k}_\phi = n_\varphi = \text{cte}$. We will write covariant components with a tilde, to distinguish them from the physical components, for which the usual notation is retained.

In terms of these variables, the ray equations are

$$(2) \quad \frac{d\psi}{d\sigma} = \frac{1}{D} \frac{\partial H}{\partial \tilde{k}_\psi} \quad \frac{d\vartheta}{d\sigma} = \frac{1}{D} \frac{\partial H}{\partial \tilde{k}_\theta}$$

$$\frac{d\tilde{k}_\psi}{d\sigma} = -\frac{1}{D} \frac{\partial H}{\partial \psi} \quad \frac{d\tilde{k}_\theta}{d\sigma} = -\frac{1}{D} \frac{\partial H}{\partial \theta}$$

$$D = \tilde{k}_\psi \frac{\partial H}{\partial \tilde{k}_\psi} + \tilde{k}_\theta \frac{\partial H}{\partial \tilde{k}_\theta}$$

On the other hand, the dispersion function H depends only on the "Stix" components k_\perp and k_\parallel , where perpendicular and parallel refer to the local direction of the static magnetic field. To relate k_\perp and k_\parallel to \tilde{k}_ψ , \tilde{k}_θ and n_p , we first introduce the physical components in the ψ, ϑ coordinates, namely

$$(3) \quad k_\psi = (\vec{k} \cdot \vec{e}_\psi) = \frac{1}{f} \left(N_c \tilde{k}_\psi - \frac{G}{N_c} \tilde{k}_\theta \right)$$

$$k_c = (\vec{k} \cdot \vec{e}_c) = \frac{1}{N_c} \tilde{k}_\theta$$

In term of these, the Stix components are easily found to be

$$(4) \quad k_\perp^2 = k_\psi^2 + k_\eta^2$$

$$k_\eta = k_c \cos(\Theta) - \frac{n_p}{R} \sin(\Theta)$$

$$k_\parallel = k_c \sin(\Theta) + \frac{n_p}{R} \cos(\Theta)$$

where $\Theta = \text{atan}(B/B_\phi)$ is given by Eq. (5-24).

With the help of Eqs. (3) and (4), writing the ray equations explicitly reduces to an exercise in implicit derivation. Since these equations constitute the core of the numerical code, we list them here in detail. For convenience, the physical components of the wave-vector are used throughout in the right-hand sides. Moreover, we use c/ω as unit of length, so that we do not distinguish between \vec{k} and $\vec{n} = c\vec{k}/\omega$.

$$(5) \quad \frac{\partial H}{\partial \tilde{k}_\perp} = 2 \frac{N_c}{f} k_\psi \frac{\partial H}{\partial k_\perp^2}$$

$$(6) \quad \frac{\partial H}{\partial \tilde{k}_\theta} = \frac{2}{N_c} \left(-\frac{G}{f} k_\psi + k_\gamma \cos \Theta \right) \frac{\partial H}{\partial k_\perp^2} + \frac{\sin \Theta}{N_c} \frac{\partial H}{\partial k_\parallel}$$

$$(7) \quad \frac{\partial H}{\partial \psi} = \frac{\partial H}{\partial k_\perp^2} \frac{\partial k_\perp^2}{\partial \psi} + \frac{\partial H}{\partial k_\parallel} \frac{\partial k_\parallel}{\partial \psi} + \sum_{\text{spec.}} \left\{ \left(\Omega \frac{\partial H}{\partial \Omega} \right) \left(\frac{1}{\Omega} \frac{\partial \Omega}{\partial \psi} \right) \right. \\ \left. + \left(n \frac{\partial H}{\partial n} \right) \left(\frac{1}{n} \frac{dn}{d\psi} \right) + \left(T \frac{\partial H}{\partial T} \right) \left(\frac{1}{T} \frac{dT}{d\psi} \right) \right\}$$

$$(8) \quad \frac{\partial H}{\partial \theta} = \frac{\partial H}{\partial k_\perp^2} \frac{\partial k_\perp^2}{\partial \theta} + \frac{\partial H}{\partial k_\parallel} \frac{\partial k_\parallel}{\partial \theta} + \sum_{\text{spec.}} \left(\Omega \frac{\partial H}{\partial \Omega} \right) \left(\frac{1}{\Omega} \frac{\partial \Omega}{\partial \theta} \right)$$

The derivatives of H are

$$(9) \quad \frac{\partial H}{\partial k_\perp^2} = 2 A n_\perp^2 - B$$

$$(9') \quad \frac{\partial H}{\partial k_\parallel} = 2 k_\parallel \left(A_\parallel n_\perp^4 - B_\parallel n_\perp^2 + C_\parallel \right)$$

$$(10) \quad A_\parallel = \frac{1}{k_\parallel^2} \left(\frac{1}{2} \lambda_\delta + \epsilon_\delta \right) \\ B_\parallel = \frac{1}{k_\parallel^2} \left\{ -n_\parallel^2 (1 + \lambda + \rho) - L_\delta \left(\frac{1}{2} + \rho \right) + R \lambda_\delta \right\} \\ C_\parallel = \frac{1}{k_\parallel^2} \left\{ 2 n_\parallel^2 (n_\parallel^2 - S) - (n_\parallel^2 - R) L_\delta \right\}$$

$$L_\delta = - \sum_j \frac{\omega_{pj}^2}{\omega^2} W(x_{1j})$$

$$(11) \quad \lambda_\delta = \frac{1}{2} \sum_j \frac{\omega_{pj}^2}{\Omega_{cj}^2} \frac{v_{thj}^2}{c^2} \left[-2 W(x_{1j}) + W(x_{2j}) \right]$$

$$\varepsilon_8 = \frac{1}{4} \sum_j \frac{\omega_{pj}^2}{\Omega_{cj}^2} \frac{v_{thj}^2}{c^2} W(x_{1j})$$

$$(12) \quad W(x_{nj}) = \frac{1}{2} \frac{\omega - n\Omega_j}{\omega} \left[x_{nj}^2 Z'(x_{nj}) + x_{nj} Z(x_{nj}) \right]$$

$$(13) \quad n_e \frac{\partial H}{\partial n_e} = -B_{ne} n_{\perp}^2 + C_{ne}$$

$$(14) \quad B_{ne} = \frac{\omega_{pe}^2}{\Omega_{ce}^2} (1 + \rho + \lambda)$$

$$C_{ne} = -2 \frac{\omega_{pe}^2}{\Omega_{ce}^2} (n_{\parallel}^2 - S)$$

$$(15) \quad n_j \frac{\partial H}{\partial n_j} = A_{nj} n_{\perp}^4 - B_{nj} n_{\perp}^2 + C_{nj}$$

$$A_{nj} = \frac{1}{2} (\rho_j + \lambda_j) + \varepsilon_j$$

$$(16) \quad B_{nj} = - \left[(n_{\parallel}^2 - L) \rho_j + (n_{\parallel}^2 - R) \lambda_j \right] + R_j \left(\frac{1}{2} + \lambda \right) + L_j \left(\frac{1}{2} + \rho \right)$$

$$C_{nj} = - \left[(n_{\parallel}^2 - R) L_j + (n_{\parallel}^2 - L) R_j \right]$$

(here and in the following $\rho_j, \lambda_j, \varepsilon_j, L_j, R_j$ denote the contribution of ion species j to $\rho, \lambda, \varepsilon, L, R$, respectively);

$$(17) \quad T_e \frac{\partial H}{\partial T_e} = 0$$

$$(18) \quad T_j \frac{\partial H}{\partial T_j} = A_{Tj} n_{\perp}^4 - B_{Tj} n_{\perp}^2 + C_{Tj}$$

$$A_{T_j} = \frac{1}{2} (\rho_j + \lambda_j) + \epsilon_j + \frac{1}{2} \lambda_{\delta_j} + \epsilon_{\delta_j}$$

$$(19) \quad B_{T_j} = -[(m_{//}^2 - R)\lambda + (m_{//}^2 - L)\rho] + \\ + R\lambda_{\delta_j} - \frac{1}{2} L_{\delta_j} (1 + 2\rho)$$

$$C_{T_j} = -(m_{//}^2 - R)L_{\delta_j}$$

$$(20) \quad \Omega \frac{\partial H}{\partial \Omega} = A_{\Omega} n_{\perp}^4 - B_{\Omega} n_{\perp}^2 + C_{\Omega}$$

$$A_{\Omega} = \frac{1}{2} (\rho_{\Omega} + \lambda_{\Omega}) + \epsilon_{\Omega}$$

$$B_{\Omega} = \frac{1}{2} (R_{\Omega} + L_{\Omega}) - [(m_{//}^2 - R)\lambda_{\Omega} + (m_{//}^2 - L)\rho_{\Omega}]$$

$$(21) \quad + R_{\Omega} \lambda + L_{\Omega} \rho$$

$$C_{\Omega} = -[(m_{//}^2 - R)L_{\Omega} + (m_{//}^2 - L)R_{\Omega}]$$

$$L_{\Omega} = -2 \frac{\omega_{pe}^2}{\Omega_{ce}^2} - \sum_j \frac{\omega_{pj}^2}{\omega^2} \left[\frac{\Omega_j}{\omega} x_{0j}^2 Z'(x_{1j}) - \frac{\omega}{\Omega_j} \right]$$

$$R_{\Omega} = -2 \frac{\omega_{pe}^2}{\Omega_{ce}^2} - \sum_j \frac{\omega_{pj}^2}{\omega^2} \left[-\frac{\Omega_j}{\omega} \left(\frac{\omega}{\omega + \Omega_j} \right)^2 + \frac{\omega}{\Omega_j} \right]$$

(22)

$$\rho_{\Omega} = -2\rho + \frac{1}{2} \sum \frac{\omega_{pj}^2}{\Omega_{cj}^2} \frac{v_{thj}^2}{c^2} \left[2 \frac{\Omega_j}{\omega} \left(\frac{\omega}{\omega + \Omega_j} \right)^2 - 2 \frac{\Omega_j}{\omega} \left(\frac{\omega}{\omega + 2\Omega_j} \right)^2 \right]$$

$$\lambda_{\Omega} = -2\lambda + \frac{1}{2} \sum \frac{\omega_{pj}^2}{\Omega_{cj}^2} \frac{v_{thj}^2}{c^2} \left[-2 \frac{\Omega_j}{\omega} x_{0j}^2 Z'(x_{1j}) + 2 \frac{\Omega_j}{\omega} x_{0j}^2 Z'(x_{2j}) \right]$$

$$\tau_{\Omega} = -2c + \frac{1}{4} \sum_j \frac{\omega_j^2}{\Omega_c^2} \frac{v_{thj}^2}{c^2} \left[\frac{\Omega_j}{\omega} x_{0j}^2 z'(x_{1j}) - \frac{\Omega_j}{\omega} x_{0j}^2 z''(x_{2j}) \right]$$

The derivatives of \vec{k} are given by

$$(23) \quad \begin{aligned} \frac{\partial k_{\perp}^2}{\partial \psi} &= 2 \left(k_{\psi} \frac{\partial k_{\psi}}{\partial \psi} + k_{\eta} \frac{\partial k_{\eta}}{\partial \psi} \right) \\ \frac{\partial k_{\perp}^2}{\partial \theta} &= 2 \left(k_{\psi} \frac{\partial k_{\psi}}{\partial \theta} + k_{\eta} \frac{\partial k_{\eta}}{\partial \theta} \right) \end{aligned}$$

$$(24) \quad \begin{aligned} \frac{\partial k_{\psi}}{\partial \psi} &= \left(\frac{1}{N_c} \frac{\partial N_c}{\partial \psi} - \frac{1}{J} \frac{\partial J}{\partial \psi} \right) k_{\psi} + \frac{1}{J} \left(\frac{2G}{N_c} \frac{\partial N_c}{\partial \psi} - \frac{\partial G}{\partial \psi} \right) k_z \\ \frac{\partial k_{\psi}}{\partial \theta} &= \left(\frac{1}{N_c} \frac{\partial N_c}{\partial \theta} - \frac{1}{J} \frac{\partial J}{\partial \theta} \right) k_{\psi} + \frac{1}{J} \left(\frac{2G}{N_c} \frac{\partial N_c}{\partial \theta} - \frac{\partial G}{\partial \theta} \right) k_z \end{aligned}$$

$$(25) \quad \begin{aligned} \frac{\partial k_{\eta}}{\partial \psi} &= -\frac{1}{N_c} \frac{\partial N_c}{\partial \psi} \cos \Theta k_z + \left(\frac{1}{R} \frac{\partial X}{\partial \psi} \right) \sin \Theta \frac{\eta_F}{R} - \frac{\partial \Theta}{\partial \psi} k_{\parallel} \\ \frac{\partial k_{\eta}}{\partial \theta} &= -\frac{1}{N_c} \frac{\partial N_c}{\partial \theta} \cos \Theta k_z + \left(\frac{1}{R} \frac{\partial X}{\partial \theta} \right) \sin \Theta \frac{\eta_F}{R} - \frac{\partial \Theta}{\partial \theta} k_{\parallel} \end{aligned}$$

$$(26) \quad \begin{aligned} \frac{\partial k_{\parallel}}{\partial \psi} &= -\frac{1}{N_c} \frac{\partial N_c}{\partial \psi} \sin \Theta k_z - \left(\frac{1}{R} \frac{\partial X}{\partial \psi} \right) \cos \Theta \frac{\eta_F}{R} + \frac{\partial \Theta}{\partial \psi} k_{\eta} \\ \frac{\partial k_{\parallel}}{\partial \theta} &= -\frac{1}{N_c} \frac{\partial N_c}{\partial \theta} \sin \Theta k_z - \left(\frac{1}{R} \frac{\partial X}{\partial \theta} \right) \cos \Theta \frac{\eta_F}{R} + \frac{\partial \Theta}{\partial \theta} k_{\eta} \end{aligned}$$

Finally, from Eqs. (3-24) and (3-25) we obtain:

$$\Theta = \arctan \frac{B_z}{B_{\phi}} = \arctan \left(\frac{a N_c}{J} Q(\psi) \right)$$

$$(27) \quad Q(\psi) = B_p(\psi) / B_0$$

$$\begin{aligned}
 (28) \quad \frac{\partial \Theta}{\partial \psi} &= \frac{\left(\frac{a N_c}{f} Q\right)}{1 + \left(\frac{a N_c}{f} Q\right)^2} \left\{ \frac{1}{N_c} \frac{\partial N_c}{\partial \psi} - \frac{1}{f} \frac{\partial f}{\partial \psi} + \frac{1}{Q} \frac{dQ}{d\psi} \right\} \\
 \frac{\partial \Theta}{\partial \theta} &= \frac{\left(\frac{a N_c}{f} Q\right)}{1 + \left(\frac{a N_c}{f} Q\right)^2} \left\{ \frac{1}{N_c} \frac{\partial N_c}{\partial \theta} - \frac{1}{f} \frac{\partial f}{\partial \theta} \right\} \\
 \frac{1}{\Omega} \frac{\partial \Omega}{\partial \psi} &= -\frac{1}{R} \frac{\partial X}{\partial \psi} + \frac{a N_c}{f} Q \frac{\partial \Theta}{\partial \psi} \\
 \frac{1}{\Omega} \frac{\partial \Omega}{\partial \theta} &= -\frac{1}{R} \frac{\partial X}{\partial \theta} + \frac{a N_c}{f} Q \frac{\partial \Theta}{\partial \theta}
 \end{aligned}$$

To the equations listed here, we must add the energy transport equation (3-9), i.e.

$$(30) \quad \frac{dP(n_\varphi)}{d\sigma} = - \frac{\gamma}{(\vec{k}_p \cdot \vec{T})} \cdot P(n_\varphi)$$

γ was given in Section 4, together with the expressions for the polarization vector, and the "Stix" components of \vec{T} . With Eqs. (3) and (4) we have also

$$\begin{aligned}
 \vec{k}_p \cdot \vec{T} &= \frac{1}{R_L} \left(k_\psi^2 + k_c k_\eta \cos \Theta \right) T_x + \\
 &\quad + k_c \sin \Theta \cdot T_z
 \end{aligned}$$

(31)

The explicit list of the equations used in the RAYIC code is thereby complete.

7. Coupling, and boundary values for ray tracing

The ray tracing code requires two pieces of information about the way IC waves are launched:

- a) the spectral decomposition of the coupled power among toroidal wavenumbers, $P(n_\phi)$;
- b) for each partial wave, the shape of a wavefront and the distribution of the power flux (Poynting vector).

On the other hand, the knowledge of the antenna impedance, which is the most complicated item in the theory of the antenna (Messiaen et al. /8/, Teilhaber and Jacquinot /9/) is not explicitly required. We have taken advantage of this fact to develop a simple model of the antenna which conveniently provides the boundary conditions for the RAYIC code.

The simplified geometry is sketched in Fig. 2: x , y , z correspond to the radial, poloidal, and toroidal directions, respectively. Our procedure consists in circumventing the evaluation of the selfconsistent current distribution in the antenna, by assuming that each element can be modeled as a section of transmission line (Fig. 2) whose inductance, capacitance and radiation resistance, L , C and R respectively, are known from the references cited above (R can be evaluated also within this model). Then the current distribution along the antenna is immediately found by solving the transmission line equations

$$(1) \quad \frac{d\bar{E}_x}{dy} = -\hat{z} \int y \quad \frac{d\int y}{dy} = -\hat{y} E_x$$

$$\hat{z} = R - i\omega L \quad \hat{y} = -i\omega C$$

with boundary conditions $E_x = 0$ at the short terminals, $[E_x] = V/(w-a)$ at the positions of the feeding coaxials, where V is the applied voltage and $w-a$ the distance antenna-wall. The current $J_y(y)$ is then a continuous function of y , with discontinuous derivatives at the coaxials feeders; in each section it is represented as a simple combination of sinusoidal functions with propagation constant

$$(2) \quad \kappa_y = \omega \sqrt{LC} \left(1 + \frac{i}{2} \frac{R}{\omega L} \right)$$

($R \ll \omega L$ is usually neglected). Assuming that the z -distribution is uniform in each element, we then easily have also the Fourier spectrum of the current distribution,

$$(3) \quad J_y(n_y, n_z) = \frac{1}{(2\pi)^2} \iint J_y(y, z) e^{-i(n_y y + n_z z)} dy dz$$

To simplify the algebra further, we assume that the distance between the antenna and the Faraday cage can be neglected, and we disregard the transverse magnetic modes ($E_z \neq 0$, $B_y = 0$) localized between the screen and the wall. These modes contribute to L and C , and, if the Faraday cage is not closed laterally, to the loading resistance of the antenna; they cannot contribute to radiation into the plasma, however. A straightforward calculation then gives the power spectrum in the form

$$(4) \quad P(n_p) = C te \cdot \sum_{n_y} |Z_b(n_y, n_z)|^2 |J_y(n_y, n_z)|^2 \operatorname{Re} Y_p(n_y, n_z)$$

$$n_z = \frac{n_p}{R}$$

Here the constant is determined from the normalization condition

$$(5) \quad \sum_{n_p} P(n_p) = P_{TOT}$$

(this step allows one to dispense with the knowledge of the antenna impedance). The form factor $Z_p(n_y, n_z)$ takes into account the geometry of the vacuum region between the wall and the plasma surface. Introducing the notation

$$(6) \quad \nu_x^2 = n_y^2 + n_z^2 - 1 \quad \nu_x = \sqrt{|\nu_x^2|}$$

Z_b can be written

$$(7) \quad \nu_x^2 < 0 \quad Z_p = - \frac{\nu_x \sin \nu_x (w-a)}{(n_z^2 - 1) \cos \nu_x w - i Y_p \nu_x \sin \nu_x w}$$

$$\nu_x^2 > 0 \quad Z_b = - \frac{\nu_x \sinh \nu_x (w-a)}{(n_z^2 - 1) \cosh \nu_x w - i Y_p \nu_x \sinh \nu_x w}$$

(w is the distance between the plasma and the wall, a the distance between the antenna and the plasma). Note that for large $n_y^2 + n_z^2 \gg 1$

$$(8) \quad Z_b \sim - \frac{\nu_x}{n_z^2 - 1} e^{-\nu_x a}$$

This exponential decrease of Z_b is due to the evanescence of these waves between the antenna and the plasma edge.

The function $Y_p(n_y, n_z)$ which appears in Eqs. (4) and (7) is the surface admittance of the plasma to plane waves,

$$(9) \quad Y_p(n_y, n_z) = \frac{B_z(n_y, n_z; x=0)}{E_y(n_y, n_z; x=0)}$$

where E_y, B_z are the solution of the cold-plasma fast-wave equations

$$(10) \quad \begin{aligned} (n_z^2 - S) \frac{dE_y}{dx} &= n_y D E_y + i(n_y^2 + n_z^2 - S) B_z \\ (n_z^2 - S) \frac{dB_z}{dx} &= -n_y D B_z - i(n_z^2 - R)(n_z^2 - L) E_y \end{aligned}$$

satisfying the appropriate radiation condition at large density (where the WKB approximation is valid):

$$(11) \quad \frac{B_z(n_y, n_z; x)}{E_y(n_y, n_z; x)} \rightarrow Y_{WKB}(n_y, n_z) = - \frac{(n_z^2 - R)(n_z^2 - L)}{(n_z^2 - S)q_x - i n_y D}$$

$$(12) \quad q_x^2 = -n_y^2 - \frac{(n_z^2 - R)(n_z^2 - L)}{(n_z^2 - S)}$$

(This condition corresponds to the assumption that all the power is absorbed in a single transit, in the spirit of ray tracing; it could however be easily modified to take into account a nonvanishing standing wave ratio within the WKB region too). In Eqs. (10)-(12) R, L, S, D are the elements of the cold plasma dielectric tensor in the notations of Stix (1961). In the code, Eqs. (10) are integrated numerically, with the same density profile as for ray tracing, but neglecting the variation of magnetic field and the rotational transform; it is of course assumed that no "resonance" $n_z^2 = S$, occurs in the near field region of the antenna.

To specify the boundary conditions completely, we have to choose an initial wavefront, Σ_0 , and the y distribution of the power flux along Σ_0 . In the present plane model, the obvious choice for Σ_0 is a plane parallel to the plasma surface. In the toroidal geometry of the code, Σ_0 has to be specified by giving the equation of its cross-section with a meridian plane, in the form

$$(13) \quad \Sigma_0: \psi = f(\vartheta) \quad \vartheta_1 \leq \vartheta \leq \vartheta_2$$

The usual choice is a strip of magnetic surface, $\psi = \text{cte}$.

It is also immediate to write the power flux distribution as a function of y (i.e. ϑ), for each partial wave with specified $n_z(n_p)$:

$$(14) \quad P_x(n_z; y) = C \cdot \text{Re} \left\{ \sum_{n_y} \sum_{n_z} Z_b^*(n_y, n_z) J_y^*(n_y, n_z) \cdot Z_b(n_y', n_z) J_y(n_y', n_z) Y_b(n_y', n_z) e^{i(n_y - n_y')y} \right\}$$

where C is a normalization constant such that $\int_{P_x} d = P(n_z)$.

8. Wave behaviour near singular surfaces

Since the Eikonal approximation often breaks down precisely where most of the absorption is expected, it is essential to investigate separately the behaviour of the waves near the singular layers. This can only be done in some details by reducing the problem to one in a single space variable. Work on these lines by M. Ottaviani and the present Author is in progress, and more detailed results will be presented elsewhere. The content of this section should be considered of a preliminary nature.

Near a two-ion hybrid resonance, the following conditions justify a simplification of the geometry to obtain a one dimensional model /10/.

- (1) The main space dependence of the dielectric tensor occurs through the variation of the magnetic field intensity B in the horizontal direction X ; the rotational transform does not play an essential role (contrary to what happens near ion-cyclotron harmonics).
- (2) The incident field can be locally assimilated to a plane wave obliquely impinging on the singular layer.

Under these conditions the wave propagation can be described by a set of ordinary differential equations in the space variable X , such as those which have been investigated in details by G. Swanson /11/. We have generalized these equations to take into account oblique incidence. More importantly, we have re-derived the hot plasma contributions, in order to resolve the ambiguity in the position of the X -derivatives /12/; thus our equations conserve the total power flux \vec{S}_k (Eq. (2-13) in the absence of dissipation.

These differential equations have to be solved, imposing the appropriate radiation conditions far from the singular layers. "Exact" solutions were obtained in two situations:

- (a) in a single species plasma near the first ion cyclotron harmonics, $\omega = 2\Omega_{ci}$. In this case the singularity is due to the confluence between the fast wave and the lowest ion Bernstein wave.
- (b) in a two species plasma near the two-ion hybrid resonance, provided that the ratio Z/A of one ion species is not an integer multiple of Z/A of the other species (e.g., He_3^{++} in a H^+ or a D^+ plasma). In this case the fast wave couples with an acoustic wave with a very short wavelength.

An approximate solution only has been obtained in the remaining case, namely

- (c) near a two-ion hybrid resonance when the fundamental cyclotron resonance of the minority species coincides with a cyclotron harmonic resonance of the main species (e.g. H^+ minority in a D^+ plasma).

These solutions (and, indeed, the differential equations themselves) are only valid when the singular layers are well separated from the Doppler-broadened cyclotron harmonic resonances. The corresponding upper limit for $|k_{||}|$ can be written /5/

$$(1) \quad |n_{||}| \lesssim \frac{\omega_{pi}^2}{\Omega_{ci}^2} \frac{V_{thi}}{c} = \beta_i \frac{c}{V_{thi}}$$

in case a), and

$$(2) \quad |n_{||}| \cdot \frac{V_{thi}}{c} \lesssim \frac{n_{\text{minority}}}{n_e}$$

in cases b) and c). Under these conditions. the power reflected and transmitted on the fast wave branch, and the power coupled to the acoustic (or Ion-Bernstein) wave can be expressed in terms of the optical thickness of the evanescence layer

$$(3) \quad \eta_1 = \frac{\pi}{2} \frac{(n_{//}^2 - R_0)^2}{(n_{//}^2 - S_0)^2} \frac{\delta + \sigma_0 n_z^2}{q_X}$$

$$(4) \quad \eta_2 = \frac{\pi}{2} \frac{(n_{//}^2 - R_0)^2}{(n_{//}^2 - S_0)^2} \sigma_0 q_X$$

Here L_0 , R_0 , S_0 are the values of L , R , S without the contribution of the minority species, n_z is the vertical component of the refractive index (which is assumed essentially constant in the singular layer), and

$$(5) \quad q_X^2 = -n_z^2 - \frac{(n_{//}^2 - R_0)(n_{//}^2 - L_0)}{(n_{//}^2 - S_0)}$$

is the (squared) horizontal component of the refractive index of the fast wave, again the absence of the minority species contribution. Finally

$$(6) \quad \delta = \frac{1}{2} \left(\frac{\omega_p^2}{\omega^2} \right)_{\text{minority}} \cdot \left(\frac{\omega}{c} R_T \right)$$

while σ_0 is zero in case b), and

$$(7) \quad \sigma_0 = \left(\frac{\omega_p^2}{\omega^2} \frac{v_{th}^2}{c^2} \right)_{\text{Main Spec.}} \cdot \left(\frac{\omega}{c} R_T \right)$$

in cases a) and c). R_T denotes here the distance from the vertical axis. Since δ is automatically zero in case a), we can express the coefficients of transmission T , reflection R , and of coupling A to the acoustic (or Ion-Bernstein) wave with a single formula for all three cases:

a') incident wave arriving on the singular layer from the low magnetic field side

$$R = [\exp(-2\eta_1) - \exp(-2\eta_2)]^2$$

$$(8) \quad T = \exp(-2(\eta_1 + \eta_2))$$

$$A = 1 + \exp(-2(\eta_1 + \eta_2)) - \exp(-4\eta_1) - \exp(-4\eta_2)$$

b') incident wave arriving on the singular layer from the high magnetic field side

$$R = 0$$

$$(9) \quad T = \exp(-2(\eta_1 + \eta_2))$$

$$A = 1 - \exp(-2(\eta_1 + \eta_2))$$

(in case a') the wave encounters first the cut-off, then the resonance, while in case b') the opposite situation occurs; wave transformation is always more efficient in the latter configuration.) Note that in both cases

$$(10) \quad R + T + A = 1$$

This is a consequence of the fact that the differential equations describing the field conserve the power flux in the absence of dissipation.

In the present version of the code, the power coupled to the acoustic wave is attributed to the electrons /13/. Of the reflected power (case a') or the transmitted power (case b'), a fraction η_Ω is absorbed by the ions at the nearby cyclotron resonance; this fraction is estimated by integrating the plane-layered limit of the power transport equation (3-9) through the cyclotron resonance.

Of course, much interest is also attached to the situation in which conditions (1) or (2) are not satisfied: in particular, in cases b) and c), this is the situation in which direct ion cyclotron heating of the minority species is expected to dominate. In the limit of strong Doppler broadening, when the singularity of the cold plasma limit is smoothed out, the code successfully integrates the ray equations through the resonance layer. Although strictly speaking the condition that the antihermitean part of the dielectric tensor should be small is violated there, it is reasonable to assume that the results are nevertheless essentially correct.

Unfortunately, the intermediate case is often encountered, in which neither the plane-layered nor ray-tracing apply. Since usually a broad range of n_{\parallel} values is launched, there is always a portion of the spectrum for which this occurs. Hence the RAYIC code in its present form is able to account only for the fate of a fraction of the launched power (cfr. next section, b)).

9. Discussion

That ray tracing cannot provide an answer to every question in connection with IC plasma heating should already be clear from the previous sections. Here we present a more systematic, albeit necessarily incomplete, discussion of the limits of this approach.

a) The most severe drawback of the ray tracing method is its inability to deal with situations in which single transit absorption is weak. The method in its present form is unable to account for the fate of that fraction of power which is either transmitted or reflected from resonance layers. It is of course conceivable to follow the reflected and transmitted rays as many times as necessary until all the power is absorbed: a set of appropriate boundary conditions is easily worked out for this purpose. This would be of little help, however, unless an estimate of the quality factors of the different n modes could also be worked out. In the weak absorption situation, even the theory of the antenna /8/, /9/ should be completely reformulated.

In the weak absorption limit, the eigenmode representation of IC waves would clearly be more appropriate. Unfortunately, such a representation has been thoroughly worked out only in cylindrical geometry, mostly with simple radial density profiles (cfr. e.g /14/). Its extension to the tokamak geometry, particularly in the presence of singular layers, is certainly a formidable problem.

In the cylindrical case, where analytic solutions are possible, it has been shown that the ray tracing and the eigenmode approaches are equivalent under very unrestrictive conditions (the first proof of this statement is due to Pekeris /15/; recently, Pekeris methods have been applied to IC waves by Connor and Colestock /16/). The results of Pekeris and Colestock suggest that a judicious application of ray tracing could help to progress also toward the understanding of eigenmode structure in more complicated geometries.

b) Ray tracing, combined with what is known about the wave behaviour near resonances, is in principle capable of predict accurately the single-transit power absorption, resolved in space and according to the particle species. It should, however, be kept in mind that the treatment of the resonance layers sketched in Section 8 is much more qualitative than the Eikonal approximation. In particular, little can be said on the transition situation, when neither the cold plasma two-ion resonance, nor the Doppler broadening of the ion cyclotron resonance dominate the wave behaviour. In spite of a long term effort, particularly by Swanson /11/, a completely satisfactory understanding of all possible situations has not yet been worked out.

c) Ray tracing is by definition inadequate to estimate diffraction effects. For example, surface waves guided between the wall and the outer plasma layers are left out of consideration. While there are some indications that such effects should be small, no quantitative estimate of their importance in the general case is available.

d) Minority and cyclotron harmonic heating lead to anisotropic supra-thermal ion populations /17/. We have taken this into account by allowing for different parallel and perpendicular temperatures. The energy gained by resonantly accelerated particles, moreover, can be thermalized partly on the electrons and partly on the ions, and can be partly lost on trapped particle orbits diffusing out of the plasma. Estimates of the relative importance of these processes can be easily made by drawing from the theory of neutral beam injection heating; Montecarlo methods have also been applied in this context /18/. A treatment of these processes is a necessary interface for the coupling of the RAYIC code to a tokamak transport code.

In conclusion, ray tracing appears to be much more useful in improving our understanding of IC waves propagation, than in making the kind of quantitative predictions ideally required by transport codes simulating tokamak discharges. Since to our knowledge no better approach to this problem is available, it is only honest to admit that many topics still await an adequate treatment. Skillful theoreticians can be kept busy for some time to come in this field.

References

- /1/ M. Brambilla, A. Cardinali, Plasma Physics 24, 1187 (1982)
- /2/ J. Jacquinet, K. Teilhaber, G. Lister, M. Brambilla, in
Proc. of the 3rd Joint Varenna-Grenoble Int.Symp. on Heating in
Toroidal Plasmas, Grenoble 1982, Vol. 1 p. 375
- /3/ S. Weinberg, Phys. Review 126, 1899,(1962)
- /4/ I.B. Bernstein, Phys. Fluids, 18, 320 (1975)
- /5/ M. Brambilla, The dispersion relation of ion cyclotron waves,
Report IPP 4/209, November 1982
- /6/ J.P. Christiansen, J.B. Taylor, Nucl. Fusion 22, 111 (1982)
- /7/ J.M. Greene, J.L. Johnson, K.E. Weimer, Phys. Fluids 14, 671 (1971)
- /8/ A. Messiaen, R. Koch, V.P. Bhatnagar, M.P. Evrard, M. Luwel,
P.E. Vandenplas, R.R. Weynants, in Proc. 3rd Joint Varenna-Grenoble
Int. Symp. on Heating in Toroidal Plasmas, Grenoble 1982,
Vol. 1 p. 243
- /9/ K. Teilhaber, J. Jacquinet, Variational theory of the ICRH antenna,
Report EUR-CEA-FC 1166, November 1982 (to be published in Nucl. Fusion)
- /10/ F.W. Perkins, Nucl. Fusion 17, 1197 (1977)
- /11/ D.G. Swanson, in Proc. 3rd Joint Varenna Grenoble Int. Symp. on
Heating in Toroidal Plasmas, Grenoble 1982, Vol. 1 p. 285
- /12/ T.H. Stix, D.G. Swanson, in Handbook of Plasma Physics Vol. 1
(A. Galeev, R.N. Sudan, Eds.), North-Holland Publ. Comp.
Amsterdam (to be published)
- /13/ J. Jacquinet, B.D. McVey, J.E. Scharer, Phys.Rev.Letters 39, 88(1977)
- /14/ J.C. Hosea, R.M. Sinclair, Phys. Fluids 13, 701 (1970)
- /15/ C.L. Pekeris, Proc. Symp. Appl. Math. 2, 71 (1950)

- /16/ K.A. Connor, P.L. Colestock, Proc. Vth Topical Conf. on RF Plasma Heating, Madison 1983, to be published
- /17/ T.H. Stix, Nucl. Fusion 15, 737 (1975)
- /18/ B. Gagey, Y. Lapierre, D. Marty, Proc. 3rd Joint Varenna-Grenoble Int. Symp. on Heating in Toroidal Plasmas, Grenoble 1982, Vol. 1 p. 361.

Figure Captions

Fig. 1: ψ, ϑ coordinates and magnetic surface cross-section in a meridian plane.

Fig. 2: Model of an antenna element as a strip of transmission line.

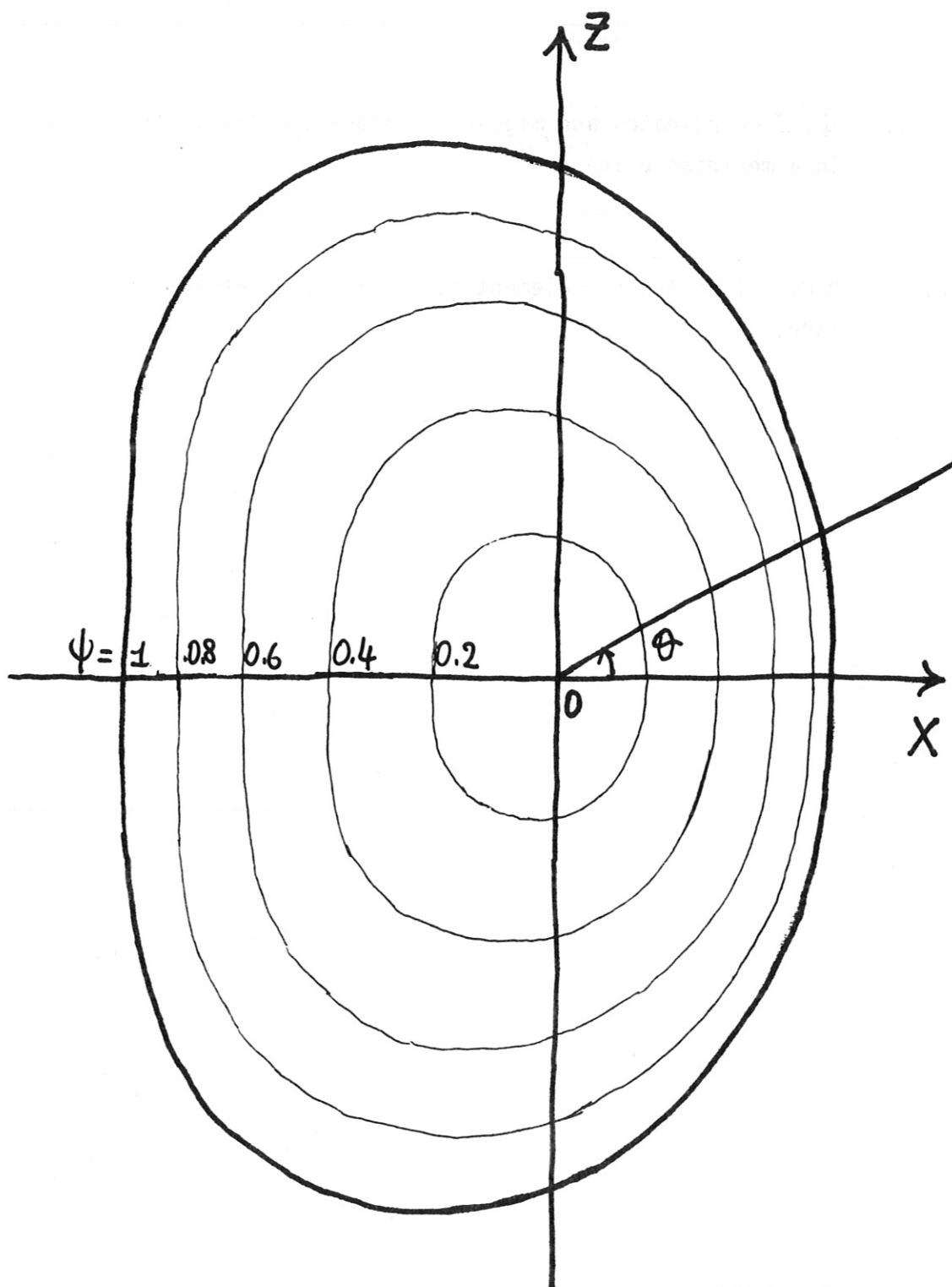


FIG. 1

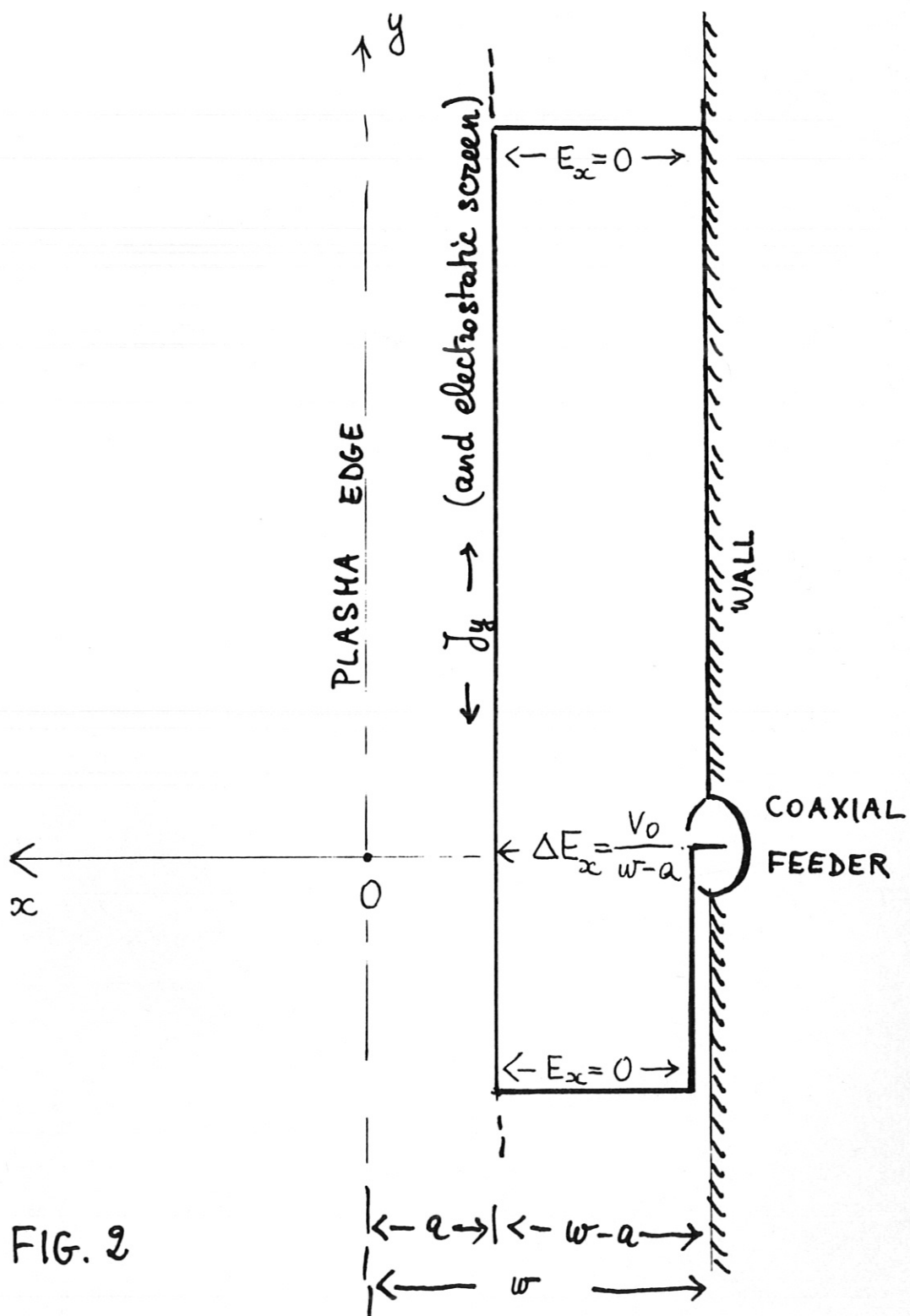


FIG. 2